ESC European Society of Cardiology

Cardiovascular Research (2018) **114**, 168–179
doi:10.1093/cvr/cvx180

LncRNA TUG1 sponges miR-204-5p to promote osteoblast differentiation through upregulating Runx2 in aortic valve calcification

Cong Yu[1,2†], Lifu Li[3†], Fei Xie[2†], Shichao Guo[2], Fayuan Liu[2], Nianguo Dong[2], and Yongjun Wang[2*]

[1]Department of Vascular Surgery, Zhejiang Provincial People's Hospital, Hangzhou 310003, Zhejiang Province, China; [2]Department of Cardiovascular Surgery, Union Hospital of Tongji Medical College, Huazhong University of Science and Technology, Wuhan 430022, Hubei Province, China; and [3]Department of Cardiovascular Surgery, Guangdong Cardiovascular Institute, Guangdong General Hospital, Guangdong Academy of Medical Sciences, Guangzhou 510080, Guangdong Province, China

Received 8 February 2017; revised 20 June 2017; editorial decision 14 July 2017; accepted 1 September 2017; online publish-ahead-of-print 4 September 2017

Time for primary review: 50 days

Aims Emerging evidence indicates that long non-coding RNAs (lncRNAs) play a vital role in cardiovascular physiology and pathology. Although the lncRNA TUG1 is implicated in atherosclerosis, its function in calcific aortic valve disease (CAVD) remains unknown.

Methods and results In this study, we found that TUG1 was highly expressed in human aortic valves and primary valve interstitial cells (VICs). Moreover, TUG1 knockdown induced inhibition of osteoblast differentiation in CAVD both *in vitro* and *in vivo*. Mechanistically, silencing of TUG1 increased the expression of miR-204-5p and subsequently inhibited Runx2 expression at the post-transcriptional level. Importantly, TUG1 directly interacted with miR-204-5p and downregulation of miR-204-5p efficiently reversed the suppression of Runx2 induced by TUG1 short hairpin RNA (shRNA). Thus, TUG1 positively regulated the expression of Runx2, through sponging miR-204-5p, and promoted osteogenic differentiation in CAVD.

Conclusion All together, the evidence generated by our study elucidates the role of lncRNA TUG1 as a miRNA sponge in CAVD, and sheds new light on lncRNA-directed diagnostics and therapeutics in CAVD.

Keywords Long non-coding RNA • TUG1 • miR-204-5p • Runx2 • Calcific aortic valve disease

1. Introduction

Calcific aortic valve disease (CAVD) is highly prevalent among adult populations worldwide with significant morbidity and mortality, and currently there are no effective medical therapies to prevent or slow the disease process.[1] Calcification of the aortic valve is now recognized as an actively regulated disease process that involves the coordinated actions of resident valve endothelial cells (VECs) and valve interstitial cells (VICs), bone marrow-derived cells, and circulating inflammatory and immune cells.[2] Normally quiescent VICs in the aortic valve leaflet become activated and undergo a phenotype transition to become osteoblast-like cells, which has been shown to contribute to calcification of the valve leaflets in CAVD.[3,4] Thus, strategies to effectively prevent transformation of VICs by inhibiting osteoblast differentiation may lead to novel therapeutic interventions to halt the progression of, or even reverse CAVD.

The sequencing of the human genome suggests that protein-coding RNA accounts for only 2% of our genome, whereas the majority of the genome remains either untranscribed or (more often) transcribed to non-protein-coding RNAs, of which functional importance has not yet been fully investigated.[5] Long non-coding RNAs (lncRNAs) are a class of transcripts longer than 200 nucleotides in length with very limited or no protein coding potential.[6] Recently, studies have shown that lncRNAs can shuttle to various subcellular locations,[7] show cell type-specific expression,[8] and play critical roles in diverse biological processes including cellular development and differentiation.[9,10] However, in the cardiovascular system, the exact role of lncRNAs under normal and pathological conditions has just begun to be uncovered.[11–13] LncRNA Chast was recently shown to promote cardiac remodelling in mice,[14] whereas another lncRNA, Chaer, defined an epigenetic checkpoint in cardiac hypertrophy.[15] Thus, studies on the biological role and underlying

* Corresponding author. Department of Cardiovascular Surgery, Union Hospital of Tongji Medical College, Huazhong University of Science and Technology, 1277 Jiefang Ave., Wuhan 430022, Hubei Province, China. Tel: +86 27 8535 1677; fax: +86 27 8365 1611, E-mail: wangyongjundoc@hotmail.com

† These authors contributed equally to the study.

molecular mechanism of lncRNAs may open up opportunities for the development of new therapeutic targets in cardiovascular diseases.

Taurine Upregulated Gene 1 (TUG1), a novel lncRNA with 6.7-kb nucleotides, is located at chromosome 22q12, and contributes to the proper formation of photoreceptors in the developing rodent retina.[16] Increasing evidence suggests that the dysregulation of TUG1 participates in the development of several cancers, such as gastric cancer, small cell lung cancer, and hepatocellular carcinoma.[17,18] It has been also reported that tanshinol could reduce atherosclerotic lesions in ApoE$^{-/-}$ mice by inhibiting TUG1, indicating the therapeutic potential of TUG1 in vascular calcification.[19] Nonetheless, limited knowledge is available on how TUG1 acts at the molecular level and its exact role in aortic valve calcification.

In recent years, a growing body of evidence demonstrates that lncRNAs modulate gene expression at different levels, including chromatin modification, transcriptional, and post-transcriptional regulation.[20,21] Moreover, a new regulatory mechanism with lncRNAs acting as a 'sponge' to titrate miRNAs, thus participating in post-transcriptional processing, has recently been identified.[22] In the study by Katsushima *et al.*,[23] TUG1 maintained the stemness features of glioma cells by sponging miR-145 in the cytoplasm. Recently, Cai *et al.*[24] reported that TUG1 can act as a molecular sponge of miR-299 to enhance tumor-induced angiogenesis in human glioblastoma. However, the miRNA sponge role of TUG1 in CAVD has not been reported yet. This prompted us to explore the interaction between TUG1 and miRNAs in human CAVD.

In our present study, we found that TUG1 was significantly upregulated in calcified aortic valves and primary human aortic VICs. Subsequent functional studies revealed that TUG1 silencing results in inhibition of osteogenic differentiation in CAVD both *in vitro* and *in vivo*. Mechanistically, TUG1 acts as a miRNA sponge to positively modulate the expression of Runx2 through sponging miR-204-5p. Therefore, our study provides new insights into the molecular function of the TUG1/miR-204-5p/Runx2 signalling pathway in the pathogenesis of CAVD and highlights the potential of lncRNAs to act as new therapeutic targets in CAVD.

2. Methods

(Expanded methods are available in the Supplementary material online).

2.1 Clinical samples

A total of 40 calcified aortic valves and their pair-matched adjacent normal tissues were explanted from patients with CAVD between 2015 and 2016 at the Department of Cardiovascular Surgery, Union Hospital, affiliated to Tongji Medical College. The patients' clinical characteristics are shown in Supplementary material online, *Table S1*. Exclusion criteria included rheumatic aortic valvulopathy, congenital valve disease, and infective endocarditis. All the studies involving humans complied with the Declaration of Helsinki and were approved by the Tongji Medical College Institutional Review Board, Huazhong University of Science and Technology. Written informed consent was obtained from the patients before surgery.

2.2 Cell culture

To isolate human aortic VICs, noncalcified aortic valves were obtained from patients undergoing heart transplant procedures. The clinical characteristics of patients are shown in Supplementary material online, *Table S2*. Primary VICs were isolated and purity of the cell preparation was confirmed as described previously.[25] Cells between passages 3 to 7 were chosen for further experiments, and incubated with an osteogenic induction medium to stimulate osteogenic differentiation as previously described.[26] All experiments involving VICs were performed on cells from independent batches.

2.3 RNA extraction and quantitative real-time polymerase chain reaction (qRT-PCR)

Total RNA was isolated using Trizol reagent (Invitrogen Corporation, Carlsbad, CA), and then reverse transcribed using a reverse transcription kit PrimeScript RT reagent Kit (Takara, Otsu, Japan) or commercial miRNA reverse transcription PCR kit (RiboBio). Quantitative real-time polymerase chain reaction (qRT-PCR) analysis was run on an ABI Step1 Plus Real Time PCR machine (Applied Biosystems, Foster City, CA) using the SYBR Premix Ex Taq kit (Takara Biomedical Technology).

2.4 Immunofluorescence staining

After treatment, VICs were collected, fixed in 4% paraformaldehyde for 10 min, and subsequently permeabilized with 0.5% Triton X-100 for another 10 min. The cells were then treated with a primary antibody against Runx2 (1:50; Santa Cruz), followed by incubation with fluorescent-conjugated secondary antibody (1:150; Abcam). Images were taken with a fluorescence microscope (Carl Zeiss, Jena, Germany) and merged using Image Pro-Plus software (Media Cybernetics, Bethesda, MD). The fluorescence intensity was assessed using Image Analysis Software and MetaMorph Microscopy Automation (Molecular Devices, Sunnyvale, CA).

2.5 RNA fluorescence *in situ* hybridization (RNA-FISH) assay

RNA-FISH Cy3-labelled TUG1 was purchased from RiboBio (Guangzhou, China). RNA-FISH assays were conducted using fluorescent *in situ* hybridization kit (RiboBio) according to the manufacturer's instructions.

2.6 Luciferase reporter assay

VICs were transfected with the full-length Runx2 promoter reporter vector (RiboBio) or human Runx2 3′-untranslated region (3′-UTR) fragment containing putative miR-204-5p binding sites for reporter vector (RiboBio). Luciferase activity was consecutively detected using the Dual-Luciferase Reporter Assay System (Promega, Madison, WI, USA). The ratio of Firefly to Renilla luciferase activity was determined to eliminate the variation in the transfection efficiencies.

2.7 RNA pull-down assay

The DNA fragment containing the full-length sequence of TUG1 or negative control sequence was amplified by PCR with a T7-containing primer, and subsequently cloned into the plasmid vector GV394 (Genechem). The resultant plasmids were linearized by digestion with restriction enzyme XhoI. Biotin-labelled RNAs were reversely transcribed using T7 RNA polymerase (Takara Biomedical Technology) and Biotin RNA Labelling Mix (Roche, USA). After treatment with RNase-free DNase I (Roche) and RNeasy Mini Kit (Qiagen, USA), the bound RNAs were isolated for further qRT-PCR assays according to the previously described method.[27]

2.8 RNA-binding protein immunoprecipitation (RIP) assay

RIP experiments were conducted using the EZ-Magna RIP Kit (Millipore Corporation, Billerica, MA). Briefly, VICs were harvested, lysed and then reacted with RIP buffer containing magnetic beads conjugated with human anti-Ago2 antibody (Millipore) or corresponding negative control IgG (Millipore). After the antibody was recovered using protein A/G beads, TUG1 and miR-204-5p levels in the precipitates were determined by qRT-PCR analysis.

2.9 Animal experiments

Adult ApoE$^{-/-}$ mice (C57BL/6 background) aged 6–8 weeks were housed in a pathogen-free, temperature-controlled environment under a 12:12 h light-dark cycle, and fed a 0.2% high cholesterol diet for 24 weeks to develop aortic valve calcification as described previously.[28] GapmeR TUG1 or GapmeR negative control (20 mg/kg) in saline was then delivered twice a week by intraperitoneal injection for another 10 weeks. At the end of the protocol, echocardiographic parameters were assessed by transthoracic echocardiography using a 18∼38 MHZ phased-array probe (MS400) connected to a Vevo 1100 Imaging system under 2.5% isoflurane anaesthesia. Following final transthoracic echocardiography, mice were euthanized by intravenous injection of a lethal dose of pentobarbital sodium (100 mg/kg), and aortic valves were removed for further biochemical analysis, including haematoxylin and eosin (H&E), as well as Alizarin Red staining. TUG1 expression in aortic valves was measured in paraffin-embedded samples using an ISH optimization kit (Roche, Basel, Switzerland) according to the manufacturer's instructions. All procedures involving animals were approved by the Institutional Animal Research Committee of Tongji Medical College, and in accordance with the European Communities Council Directive 2010/63/EU for the protection of animals used for experimental purposes.

2.10 Detection of glucose, total cholesterol (TC), low density lipoproteins (LDLs), and triglyceride (TG) levels

Animals were subjected to a 14–15 h fast before blood samples were collected. Serum glucose, TC, LDLs, and TG levels were measured using indicated kits (Biosino Biotechnology Company Ltd, China).

2.11 Statistical analysis

Statistical analyses were performed using GraphPad Prism 5 software (La Jolla, CA). Data are presented as mean ± SEM, and analysed using the Student's *t*-test (when 2 groups were compared) or analysis of variance followed by Bonferroni's test (when >2 groups were compared). The association of the two variables was evaluated using a two-tailed Pearson's correlation analysis. For *in vitro* assays with human aortic VICs, n represents the number of experiments performed in different donors. $P < 0.05$ was considered to be statistically significant.

3. Results

3.1 TUG1 is highly expressed in CAVD and is associated with osteoblast differentiation of VICs

To assess whether TUG1 expression was altered in CAVD, we performed qRT-PCR for RNA in 40 pairs of calcified aortic valves and adjacent normal tissues (see Supplementary material online, *Table S1* for details on patient characteristics). The qRT-PCR results show that the level of TUG1 mRNA was significantly upregulated in calcified aortic valves compared with normal tissues ($P < 0.05$, *Figure 1A*). Moreover, high levels of TUG1 were also detected in primary human aortic VICs compared with several cell lines, including HEK-293 T, COS7, and primary VECs (*Figure 1B*). We next isolated human aortic VICs from non-calcified aortic valves (heart transplantation) (see Supplementary material online, *Table* S2 for details on patient characteristics), and confirmed by RNA fluorescent *in situ* hybridization (RNA-FISH) that TUG1 was localized predominantly in the cell cytoplasm but not in the nucleus (*Figure 1C*). Since VICs undergo a phenotype transition to become osteoblast-like cells in CAVD,[3] we then investigated whether TUG1 was involved in osteoblastic differentiation of VICs. As shown in *Figure 1D*, expression of TUG1 was induced upon stimulation of VICs with osteogenic medium. In addition, we also found that the level of TUG1 mRNA was strongly positively correlated with three known osteoblastic differentiation markers (ALP, osteocalcin, and osteopontin) mRNA levels at 0, 1, 3, 5, 7, and 14 days after osteogenic induction of VICs ($P < 0.01$, *Figure 1E*). These data indicate that TUG1 may participate in CAVD progression through its association with osteoblast differentiation of VICs.

3.2 Knockdown of TUG1 inhibits osteogenic medium-induced osteoblast differentiation *in vitro*

Given that TUG1 is overexpressed in calcified aortic valves and associated with osteoblast differentiation of VICs, we performed *in vitro* gain- and loss-of-function experiments in VICs to investigate whether TUG1 could reprogram VICs toward an osteogenic phenotype. Three short hairpin RNAs (shRNAs) targeting the coding region of TUG1 (shTUG1) were tested for their knockdown efficiency. The most efficient two, shTUG1-1 and shTUG1-2, (*Figure 2A*) were chosen for further experiments. VICs transfected with shTUG1-1, shTUG1-2 or negative control (sh-NC) were cultured in osteogenic medium to induce osteoblast differentiation, and then collected to detect ALP activity, calcified nodule formation and protein levels of osteoblastic differentiation markers (osteocalcin, osteopontin, and osterix). The results showed that shRNA-mediated silencing of TUG1 in VICs negated the osteogenic differentiation medium-induced increase in ALP activity (*Figure 2C*), calcified nodule formation (*Figure 2E*), and the protein levels of osteoblastic differentiation markers (*Figure 2G*) compared with control cells. In contrast, overexpression of TUG1 (*Figure 2B*) resulted in further increases in ALP activity (*Figure 2D*), calcified nodule formation (*Figure 2F*), and the protein levels of osteoblastic differentiation markers (*Figure 2H*) in VICs. These results indicate that TUG1 plays a positive role in osteoblast differentiation of VICs.

3.3 TUG1 directly interacts with miR-204-5p

As a newly described regulatory mechanism, a cytoplasmic lncRNA can act as a natural miRNA sponge, which interferes with miRNA pathways and reduces binding of endogenous miRNAs to target genes at the post-transcriptional level.[29] Using an online bioinformatics database (FINDTAR3, http://bio.sz.tsinghua.edu.cn/and RNAhybrid), we found that miR-30 b-5p, miR-125 b-5p, miR-148a-3p miR-204-5p, and miR-214-3p have putative binding sites with TUG1 (*Figure 3A*). To further verify which miRNAs TUG1 could directly interact with, a biotin-labelled pull-down assay was performed. The TUG1 pulled down pellet contained a significant amount of miR-204-5p, analysed by qRT-PCR,

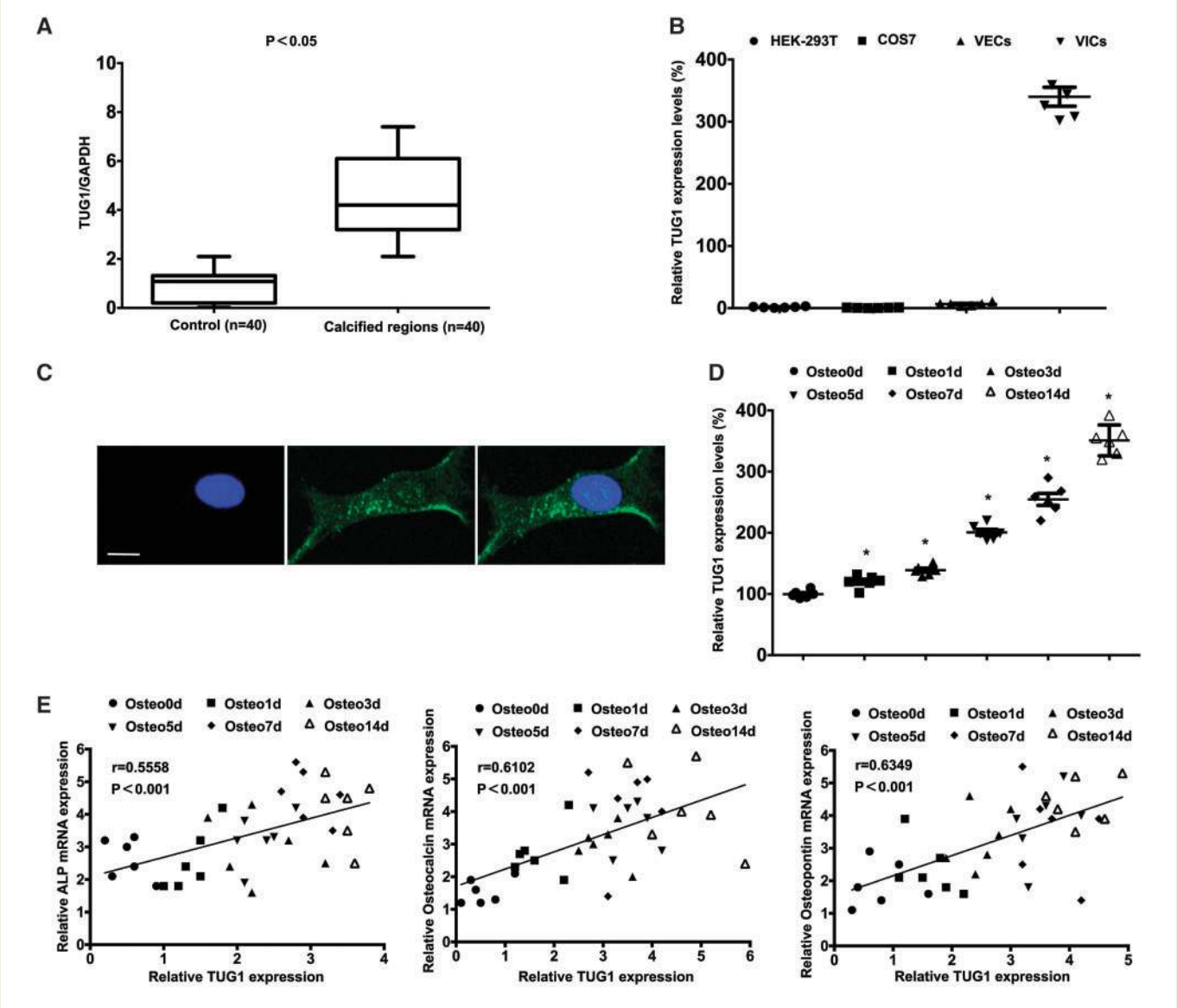

Figure 1 TUG1 is highly expressed in calcific aortic valve disease (CAVD) and associated with the osteoblast differentiation of primary aortic valve interstitial cells (VICs). (*A*) Expression level of TUG1 in calcified aortic valves and adjacent normal tissues ($n = 40$). (*B*) TUG1 expression in cell lines and VICs ($n = 6$). (*C*) RNA fluorescent *in situ* hybridization (FISH) for TUG1 in isolated VICs ($n = 6$). Scale bar 10 μM. (*D*) TUG1 expression in VICs 0, 1, 3, 5, 7, and 14 days after osteogenic induction ($n = 6$). (*E*) Correlation analysis between TUG1 and osteoblastic differentiation markers (ALP, osteocalcin, and osteopontin) mRNA levels in VICs 0, 1, 3, 5, 7, and 14 days after osteogenic induction ($n = 6$). Values are mean ± SEM. *$P < 0.05$ vs. control.

whereas the amount of miR-30 b-5p, miR-125 b-5p, miR-148a-3p, and miR-214-3p did not increase when compared to controls (*Figure 3B* and *C*). It has been shown that miRNAs exert their gene silencing through the RNA-induced silencing complex (RISC), and that Ago2 is the core component of the RISC.[30] To test if TUG1 and miR-204-5p are in the same RISC, we performed a RIP assay and found that higher TUG1 and miR-204-5p RNA levels were detected in Ago2 immunoprecipitates relative to control IgG immunoprecipitates (*Figure 3D*). These results support the bioinformatics predictions indicating that TUG1 could directly sponge miR-204-5p.

3.4 Knockdown of TUG1 increases the expression of miR-204-5p, and inhibits the expression of Runx2

To determine whether the expression of miR-204-5p is regulated by TUG1, we transfected VICs with shTUG1-1, shTUG1-2 or pcDNA-TUG1. After knockdown of TUG1, expression of miR-204-5p was significantly upregulated (*Figure 4A*). On the contrary, overexpression of TUG1 led to significant knockdown of miR-204-5p expression (*Figure 4B*). Whereas, the expression levels of miR-21-5p, miR-125 b-5p,

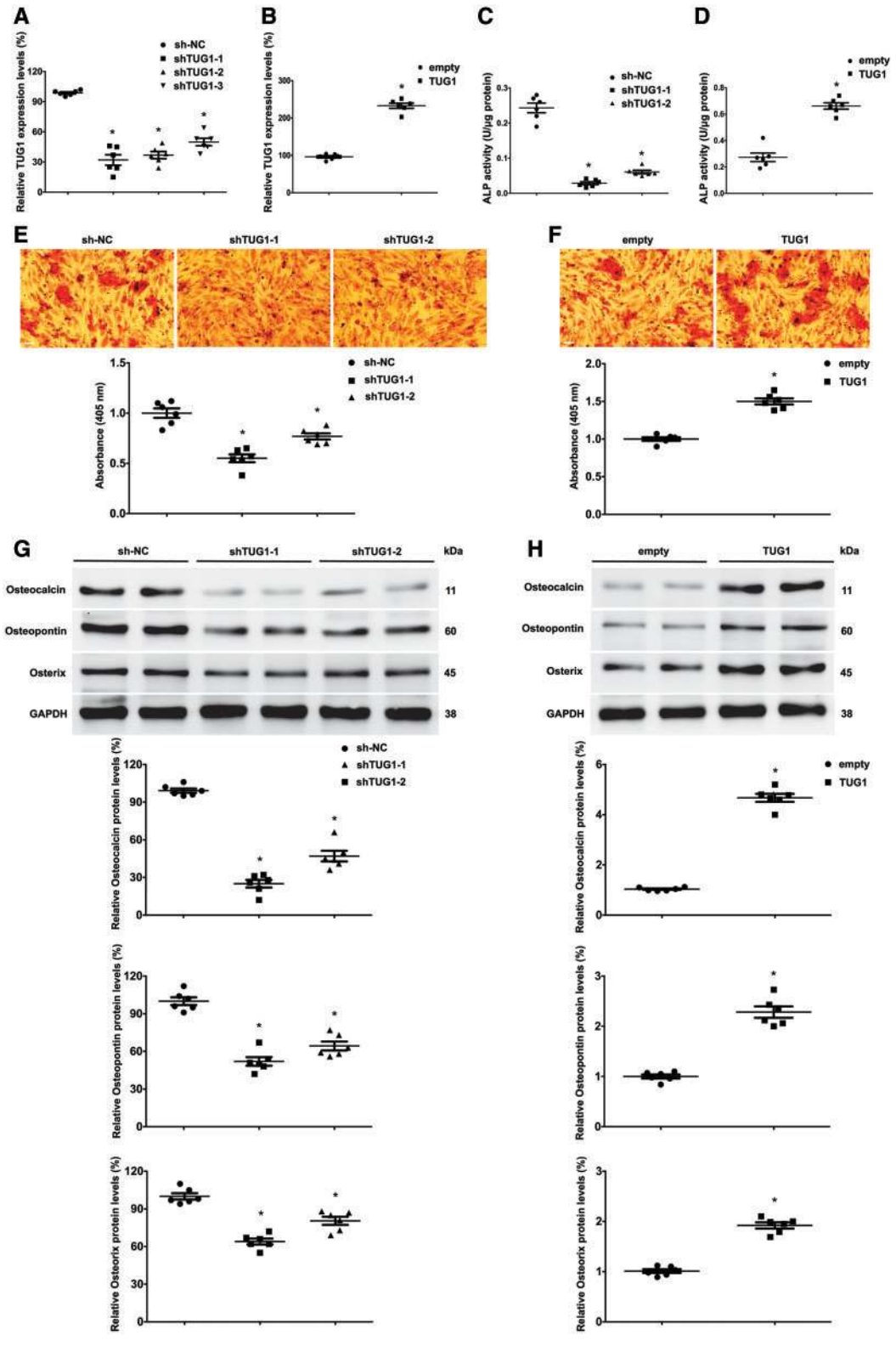

Figure 2 Knockdown of TUG1 inhibits osteogenic medium-induced osteoblast differentiation *in vitro*. (*A*) Silencing of TUG1 with shRNAs in VICs ($n = 6$). (*B*) The expression of TUG1 increased in VICs transfected with GV144-TUG1 ($n = 6$). (*C* and *D*) Human VICs were transfected with two shRNAs (shTUG1-1 and shTUG1-2) or GV144-TUG1, and stimulated with osteogenic differentiation medium for 7 days. ALP activities were evaluated by spectrophotometry ($n = 6$). (*E* and *F*) Mineralized bone matrix formation was evaluated by Alizarin Red staining ($n = 6$), scale bar 50 μM. (*G* and *H*) Representative western blots and quantification of osteoblastic differentiation markers (osteocalcin, osteopontin, and osterix) protein levels were measured by western blot ($n = 6$). GAPDH was used for normalization. Values are mean ± SEM. *$P < 0.05$ vs. sh-NC or empty.

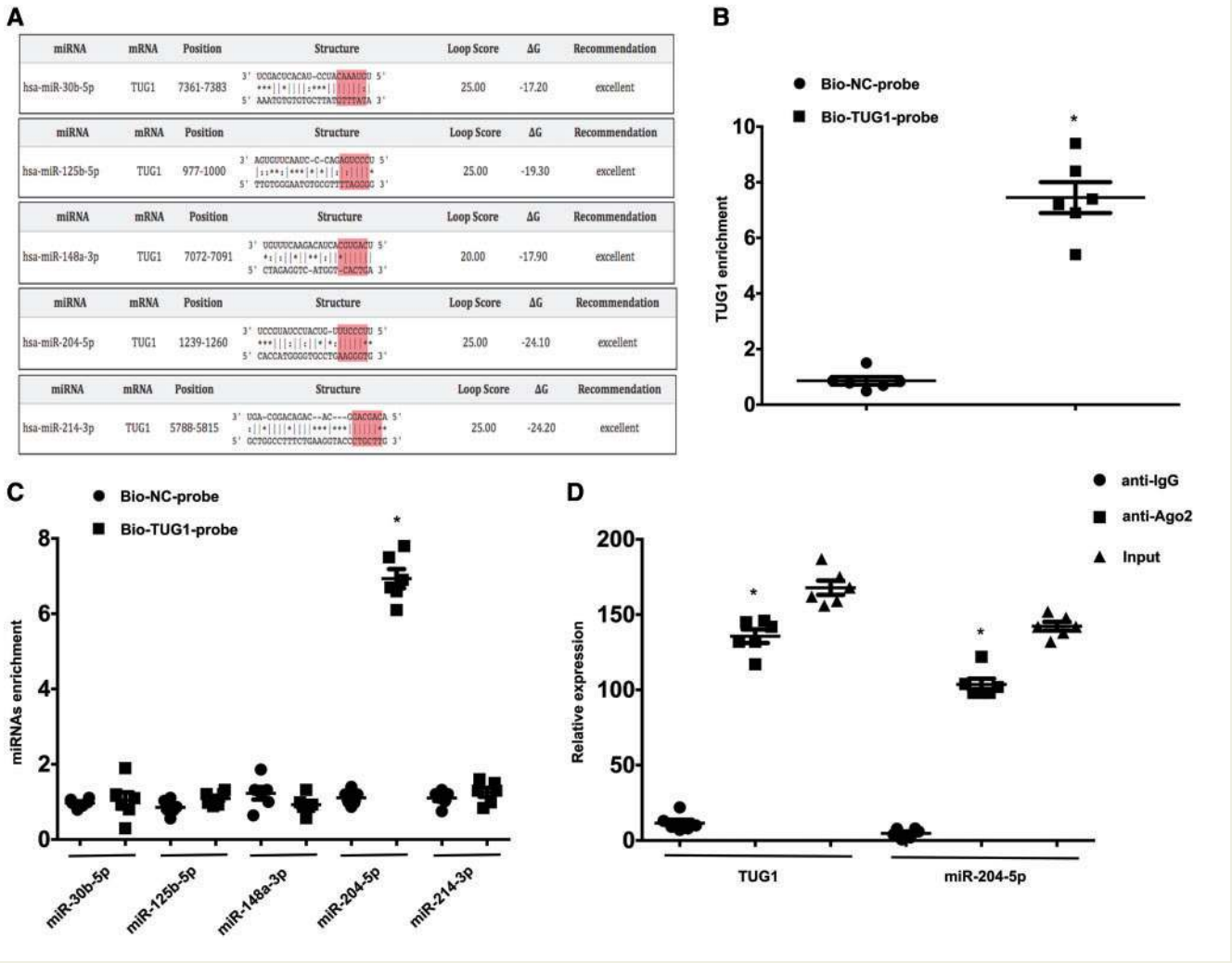

Figure 3 TUG1 directly interacts with miR-204-5p. (*A*) Putative binding sites of TUG1 with miR-30 b-5p, miR-125 b-5p, miR-148a-3p miR-204-5p, and miR-214-3p, as predicted by FINDTAR3. (*B*) Detection of TUG1 using quantitative reverse transcription-polymerase chain reaction (qRT-PCR) in the same sample pulled down by the biotinylated TUG1 and negative control (NC) probe ($n = 6$). *$P < 0.05$ vs. Bio-NC-probe. (*C*) Detection of miR-30 b-5p, miR-125 b-5p, miR-148a-3p miR-204-5p, and miR-214-3p using qRT-PCR in the sample pulled down by the biotinylated TUG1 and NC probe. Input was used for normalization ($n = 6$). *$P < 0.05$ vs. Bio-NC-probe. (*D*) RNA-binding protein immunoprecipitation (RIP) assays were performed using input from cell lysate, normal mouse IgG or anti-Ago2. Relative expression levels of TUG1 and miR-204-5p in VICs were detected by qRT-PCR ($n = 6$). Values are mean ± SEM. *$P < 0.05$ vs. anti-IgG.

miR-133a-3p, and miR-155-5p had only slight changes in cells transfected with sh-TUG1 or pcDNA-TUG1 when compared with controls (data not shown). Moreover, it should be noted that TUG1 expression was not affected after knockdown or overexpression of miR-204-5p (data not shown). These results show that TUG1 regulated expression levels of miR-204-5p in VICs. Recent studies indicate that Runx2 is not only involved in bone and cartilage development but also plays an active role in osteogenic-like calcification in CAVD.[31] Subsequently, we further investigated the expression of Runx2 in cells down-regulating TUG1. Upon TUG1 inhibition, Runx2 mRNA and protein levels decreased significantly in VICs (*Figure 4C*, *E* and *G*). Conversely, Runx2 mRNA and protein levels were significantly upregulated upon TUG1 overexpression (*Figure 4D*, *F* and *H*). Moreover, TUG1 was found to correlate negatively with miR-204-5p ($r = –0.6474$, $P < 0.01$; *Figure 4I*) and positively with Runx2 ($r = 0.5011$, $P < 0.01$; *Figure 4J*) in the 40 human calcified aortic valves. These analyses show that TUG1 may play a critical role in osteogenic differentiation by targeting Runx2.

3.5 TUG1 positively regulates post-transcriptional expression of Runx2 through miR-204-5p *in vitro*

To confirm the effect of miR-204-5p on Runx2, human Runx2 3′-UTR fragments containing putative binding sites for the miR-204-5p reporter vector and the Runx2 promoter reporter vector were used in Dual-luciferase Reporter Assays. The results indicate that shRNA-mediated silencing of TUG1 significantly decreased the relative Runx2 3′-UTR luciferase activity in VICs (*Figure 4K*). Conversely, luciferase activity significantly increased in the cells transfected with GV-144-TUG1 (*Figure 4L*). However, there was only a slight change in the promoter activity of Runx2 upon TUG1 inhibition or overexpression in VICs (*Figure 4M*).

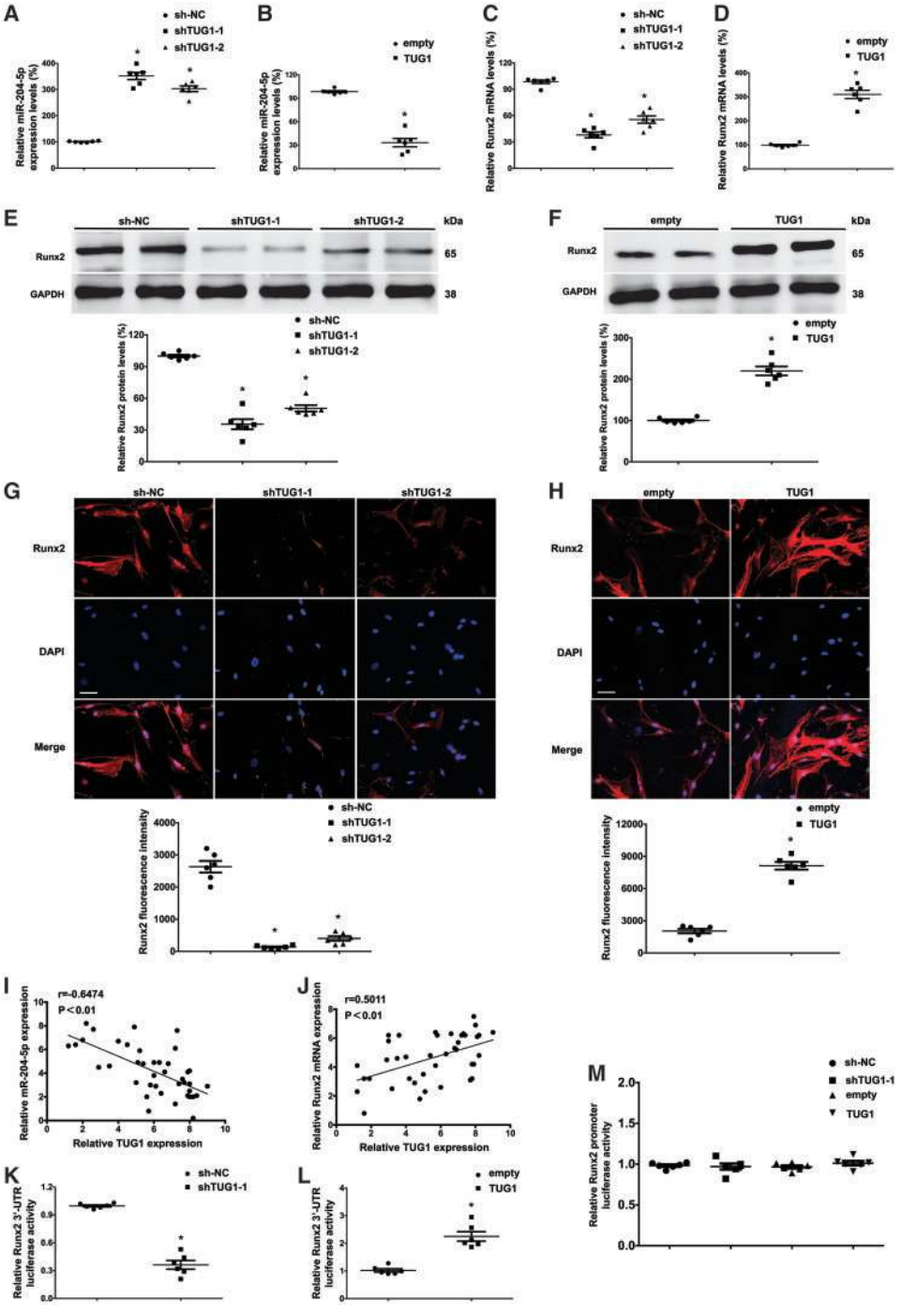

Figure 4 The effect of TUG1 on the expression levels of miR-204-5p and Runx2. Human VICs were transfected with two shRNAs (shTUG1-1 and shTUG1-2) or GV144-TUG1, and stimulated with osteogenic differentiation medium for 7 days. (*A* and *B*) The expression levels of miR-204-5p were evaluated by qRT-PCR ($n = 6$). U6 was used for normalization. (*C* and *D*) The Runx2 mRNA levels (normalized to GAPDH) in VICs were detected by qRT-PCR ($n = 6$). (*E* and *F*) Representative western blots and quantification of Runx2 protein levels in VICs transfected with two shRNAs (*E*) or GV144-TUG1 (*F*) ($n = 6$). GAPDH was used for normalization. (*G* and *H*) Fluorescence-labelled Runx2 protein in VICs was visualized by fluorescence microscopy ($n = 6$). Runx2 was stained in red and nuclei in blue, scale bar 50 μM. (*I* and *J*) Correlation analysis between TUG1 and miR-204-5p (*I*), TUG1 and Runx2 (*J*) among human calcific aortic valves ($n = 40$) as indicated by two-tailed Pearson's correlation analysis. (*K* and *L*) Relative luciferase activities of Runx2 3′-untranslated regions (3′-UTR) reporter in VICs transfected with two shRNAs (*K*) or GV144-TUG1 (*L*) using the Dual-Luciferase Reporter Assay System ($n = 6$). (*M*) Relative luciferase activities of Runx2 promoter reporter in VICs transfected with shRNA or GV-144-TUG1 ($n = 6$). Values are mean ± SEM. *$P < 0.05$ vs. sh-NC or empty.

Our data indicate that TUG1 modulates the expression of Runx2 at the miR-204-5p mediated post-transcriptional level.

3.6 Knockdown of miR-204-5p reversed Runx2 level and osteoblast differentiation induced by TUG1 shRNA *in vitro*

We then explored whether knockdown of miR-204-5p could partly reverse osteoblast differentiation of VICs induced by TUG1 shRNA. As expected, overexpression of anti-miR-204-5p partly reversed ALP activity (*Figure 5A*), calcified nodule formation (*Figure 5B*), and the protein levels of osteoblastic differentiation markers in VICs (*Figure 5C*). Additionally, we also found that downregulation of miR-204-5p with anti-miR-204-5p efficiently reversed the inhibition of Runx2 protein levels induced by TUG1 shRNA in VICs (*Figure 5C* and *D*). These analyses show that TUG1 sponges miR-204-5p to promote osteoblast differentiation of VICs through upregulating Runx2.

3.7 *In vivo* targeting of TUG1 reduces high-cholesterol diet-induced aortic valve calcification in ApoE$^{-/-}$ mice

We next tested the therapeutic potential of TUG1 inhibition in an animal model of aortic valve calcification. Here, ApoE$^{-/-}$ mice were given a high cholesterol diet for 24 weeks to develop aortic valve calcification, and then were treated for 10 weeks with twice a week injections of a GapmeR against a scrambled sequence (control) or against TUG1. After 10 weeks, GapmeR-mediated silencing of TUG1 (*Figure 6A* and *B*) led to a significant increase in miR-204-5p expression in mice compared to animals treated with control-GapmeRs (*Figure 6C*). On the contrary, TUG1 inhibition significantly decreased Runx2 levels (*Figure 6D*), and the mRNA levels of osteoblastic differentiation markers (*Figure 6E–H*) in aortic valve leaflets of mice. We then assessed the morphology of the valve leaflets and the degrees of calcification. *In vivo* repression of TUG1 consistently decreased aortic valve leaflet thickness compared to mice treated with a scrambled control, assessed using haematoxylin and eosin (H&E) staining (*Figure 6I*). This is in line with decreased calcium deposits in aortic valve leaflets of animals treated with TUG1-GapmeR when compared with control-GapmeR (*Figure 6J*). Most importantly, echocardiographic assessment of hearts from mice treated with the control-GapmeR showed a significant increase in transvalvular peak jet velocity, aortic valve area (AVA) and AVA index, whereas animals treated with the TUG1-GapmeR had significantly decreased transvalvular peak jet velocity, AVA and AVA index (*Figure 6K–M*). However, there were no significant difference in left ventricular/right ventricular (LV/RV) diameters, LV systolic/diastolic function, and systemic haemodynamics parameters between groups at the time of sacrifice (see Supplementary material online, *Table* S3). Moreover, the twice a week dosing regimen did not result in significant changes in metabolic parameters, such as glucose, total cholesterol (TC), low density lipoprotein (LDL), and triglyceride (TG) (see Supplementary material online, *Table S4*). These results further verify the role of TUG1 in osteoblast differentiation and provide more evidence for a therapeutic strategy targeting TUG1 in CAVD treatment.

In this work, we demonstrated that lncRNA TUG1 sponges miR-204-5p to positively regulate Runx2 expression at the post-transcriptional level, and thereby promotes osteoblast differentiation of VICs in CAVD progression (*Figure 7*).

4. Discussion

Although evidence has shown the ectopic expression of lncRNA TUG1 in many cancers,[17,18] its expression and biological role in CAVD remain uncharacterized. Our study confirms that TUG1 expression is significantly higher in human calcified aortic valves compared with adjacent normal tissues. High TUG1 expression is also associated with osteoblast differentiation of primary human aortic VICs. Our gain- and loss-of-function experiments indicate that TUG1 could indeed promote osteoblast differentiation of primary VICs as evidenced by increased ALP activity, calcified nodule formation and expressions of osteoblast differentiation markers. Moreover, GapmeR-mediated silencing of TUG1 reduced high-cholesterol diet-induced aortic valve calcification in ApoE$^{-/-}$ mice without altering left ventricular (LV) function or metabolic parameters, by reducing leaflet hyperplasia and calcification and inhibiting osteogenic signalling. All together, these data support the concept that TUG1 functions as a positive regulator of osteoblast differentiation in CAVD progression. A new mechanism has been proposed in which stretch-mediated repression of lncRNA HOTAIR results in increased expression of calcification genes in VICs,[32] and more recently, Hadji *et al.*[33] have demonstrated that altered DNA methylation of lncRNA H19 in CAVD promotes mineralization by silencing NOTCH1. From these studies, a broader understanding of the mechanisms of action of more lncRNAs may further the development of new therapeutic strategies for CAVD.

LncRNAs has been reported to be located in both the nucleus and cytoplasm, and subcellular localization patterns of lncRNAs reveal fundamental insights into their biology and foster hypotheses for potential molecular roles.[34,35] It has been reported that TUG1 was localized in the cytoplasm and nucleus in glioma stem cells,[23] and we obtained a similar result when we performed RNA FISH assay in VICs, indicating that TUG1 might participate in post-transcriptional regulations in the cytoplasm. Recently, a novel mechanism of post-transcriptional regulation that lncRNAs function as a natural miRNA sponge, interfere with miRNA pathways, and regulate the de-repression of miRNA targets has been identified.[36] The miRNA sponge function of TUG1 is supported by the evidence generated in our study. First, TUG1, predominantly located in the cytoplasm, was highly expressed in calcified aortic valves and primary VICs and negatively correlated with miR-204-5p in tissues. Second, the expression of miR-204-5p decreased upon overexpression of TUG1, whereas miR-204-5p expression increased after depleting MALAT1 expression by either siRNAs or GapmeRs. Third, we predicted the interaction between TUG1 and miR-204-5p using an online bioinformatics database and found that TUG1 indeed contains a target site of miR-204-5p. Fourth, downregulation of miR-204-5p efficiently reversed the suppression of Runx2 and osteoblastic differentiation induced by TUG1 shRNA. Finally, we found that TUG1 could pull down miR-204-5p, and that TUG1 and miR-204-5p were in the same RISC complex. In addition to interaction with miRNAs, a single lncRNA could have multiple roles in the cytoplasm.[37] Moreover, lncRNAs could exhibit different regulatory mechanisms in the nucleus and cytoplasm.[23,38] Other functions of TUG1 in the cytoplasm and nucleus of VICs may need further investigation.

The master osteoblast transcription factor Runx2, has been closely associated with the osteoblast differentiation of VICs in CAVD.[39] Once Runx2 is expressed, VICs are committed to an osteoblast lineage, promote expression of calcification-related proteins such as osteocalcin, osteopontin and osterix, and undergo calcification.[40] Twist-related protein 1 targets Runx2 to negatively regulate osteoblast differentiation of

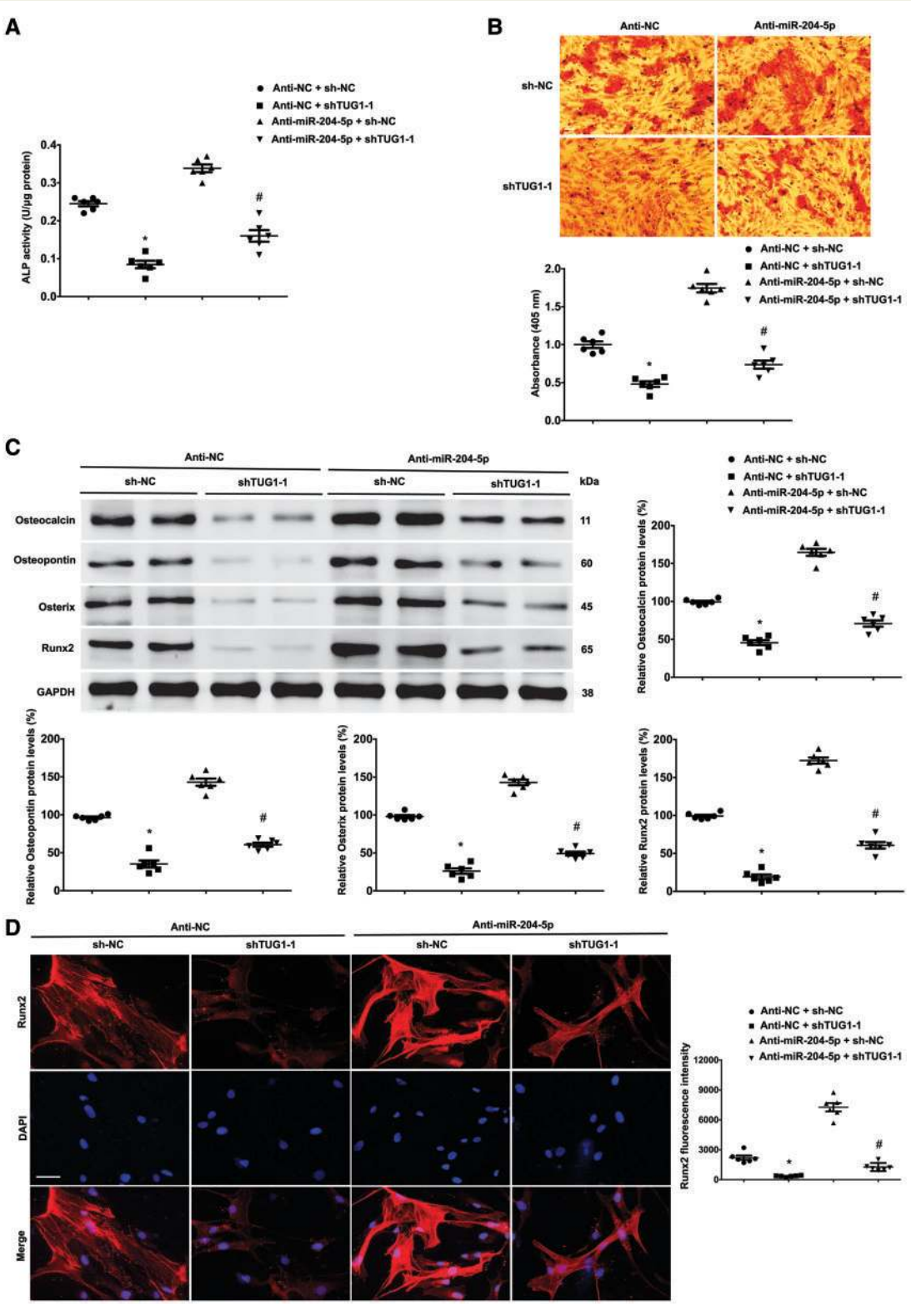

Figure 5 Knockdown of miR-204-5p reversed Runx2 levels and osteoblast differentiation induced by TUG1 shRNA *in vitro*. Human aortic VICs were transfected with TUG1 shRNA (shTUG1-1), miR-204-5p inhibitor (Anti-miR-204-5p), or their corresponding negative controls, and then stimulated with osteogenic differentiation medium for 7 days. (*A*) ALP activities were evaluated by spectrophotometry ($n = 6$). (*B*) Alizarin Red staining showed that knockdown of miR-204-5p with Anti-miR-204-5p partly reversed mineralized bone matrix formation induced by shTUG1-1 in VICs ($n = 6$), scale bar 50 μM. (*C*) Representative western blots and the quantification for Runx2, osteocalcin, osteopontin, and osterix protein expression in VICs ($n = 6$). GAPDH was used for normalization. (*D*) Fluorescence-labelled Runx2 protein in VICs was visualized by fluorescence microscopy ($n = 6$). Runx2 was stained in red and nuclei in blue, scale bar 50 μM. Values are mean ± SEM. * $P < 0.05$ vs. Anti-NC plus sh-NC; # $P < 0.05$ vs. Anti-NC plus shTUG1-1.

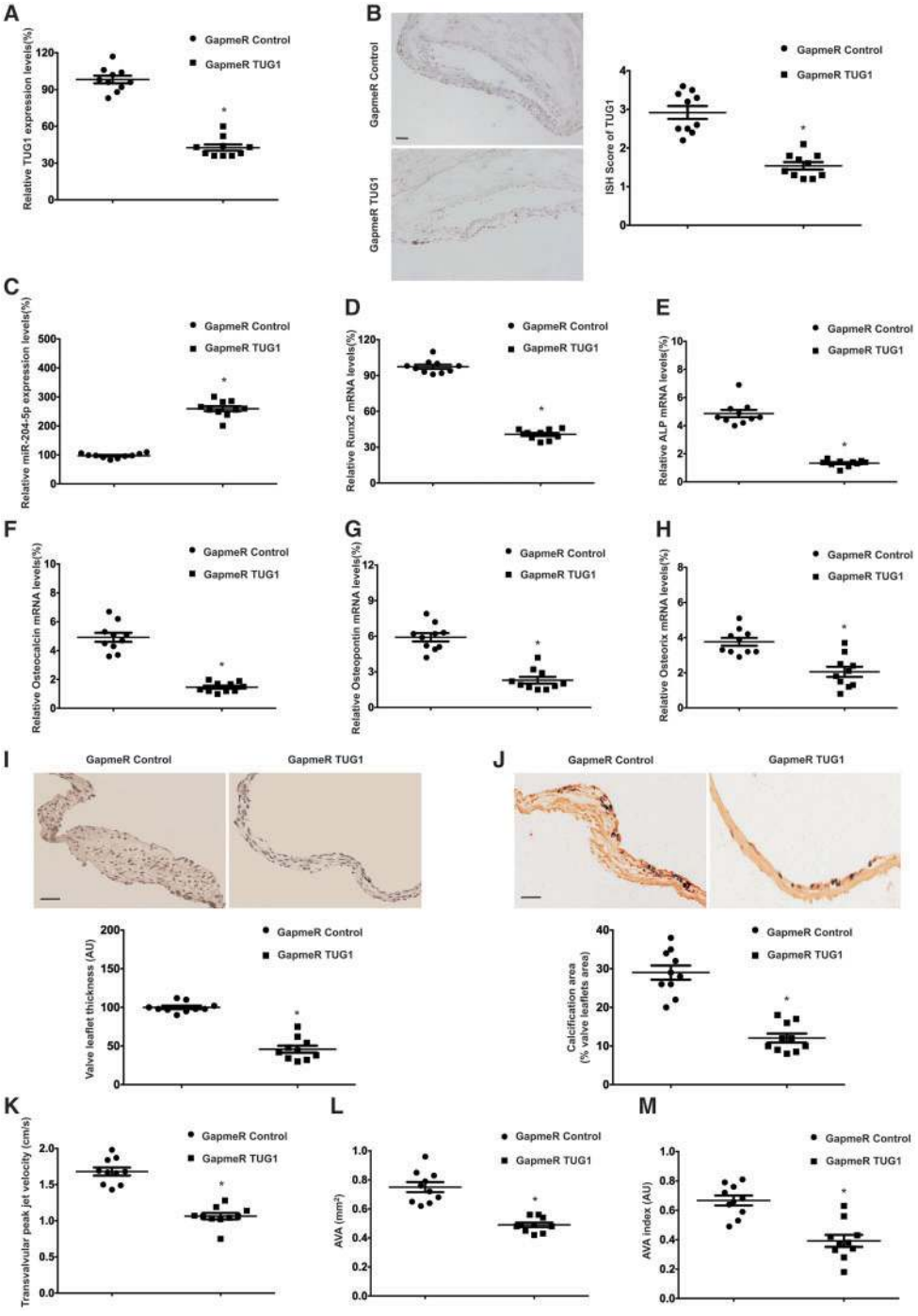

Figure 6 *In vivo* targeting of TUG1 reduces high-cholesterol diet-induced aortic valve calcification in ApoE$^{-/-}$ mice. (*A*) qRT-PCR analysis of TUG1 expressions in aortic valve leaflets of GapmeR control-treated or GapmeR TUG1-treated mice ($n = 10$/group). (*B*) Representative *in situ* hybridization (ISH) images and quantification of TUG1 in aortic valve leaflets of GapmeR control-treated or GapmeR TUG1-treated mice ($n = 10$/group). (*C–H*) Expression of miR-204-5p and Runx2, and osteoblastic differentiation marker genes (ALP, osteocalcin, osteopontin and osterix) in aortic valve leaflets of GapmeR control-treated or GapmeR TUG1-treated mice detected by qRT-PCR ($n = 10$/group). (*I*) Representative haematoxylin and eosin (H&E) staining images and quantification of leaflet thickness in GapmeR control-treated or GapmeR TUG1-treated mice ($n = 10$/group). We analysed mean aortic valve leaflet thickness and used the mean thickness of GapmeR control-treated mice as a reference against that of GapmeR TUG1-treated mice. (*J*) Alizarin Red staining was performed to evaluate the calcium deposits in valve leaflets ($n = 10$/group). (*K–M*) Echocardiographic data in GapmeR control-treated or GapmeR TUG1-treated mice: transvalvular peak jet velocity, AVA (aortic valve area) and AVA index ($n = 10$/group), scale bar 100 μM. Values are mean ± SEM. $^*P < 0.05$ compared with GapmeR controls.

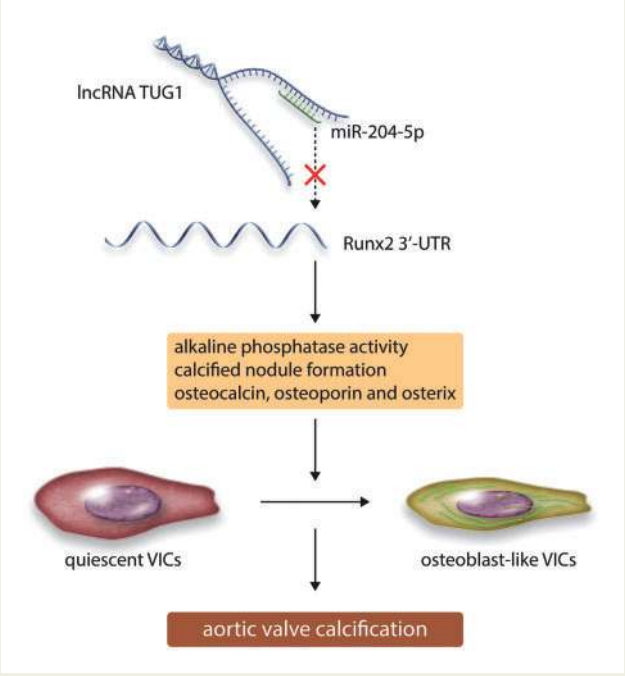

Figure 7 Graphical abstract of how long non-coding RNAs (lncRNAs) TUG1 promotes aortic valve calcification. TUG1 sponges miR-204-5p to positively regulate Runx2 expression at the post-transcriptional level, and thereby promotes osteoblast differentiation of human aortic valve interstitial cells (VICs) in progression of aortic valve calcification.

VICs,[41] and conversely, reactive oxygen species promote activation of VICs toward an osteogenic-like phenotype via upregulating Runx2,[42] suggesting that the modulation of Runx2 levels could represent an important approach for the treatment of CAVD. Our previous study also found that miR-204 directly targets Runx2 to attenuate BMP-2-induced osteoblast differentiation in VICs.[43] In the present study, we identified that TUG1 could positively regulate Runx2 expression at the post-transcriptional level through sponging miR-204-5p in VICs. In fact, it has been shown that individual protein-coding genes were modulated by multiple sponge lncRNAs, and that one sponge lncRNAs could regulate several protein-coding genes.[44,45] Thus, whether Runx2 could be regulated by other sponge lncRNAs, and whether TUG1 could function as a sponge lncRNA to affect expressions of other key regulators in CAVD, may need further investigation.

CAVD is the most prevalent form of aortic stenosis (AS) worldwide without effective pharmacotherapy. Invasive aortic valve replacement for severe AS, or less invasive transcatheter aortic valve replacement for patients at high or prohibitive risk for surgical valve replacement, remain the only curative treatments.[1] A multifaceted and active process involving lipoprotein deposition and oxidation, chronic inflammation, osteoblast differentiation of VICs and active leaflet calcification has been found to contribute to CAVD, suggesting that strategies targeting these cellular events may be used to develop novel therapeutic interventions to halt the progression of AS or even eliminate the need for valve replacement.[46] Recent studies highlight that lncRNAs play a prominent role in modulation of osteoblast differentiation in many cell lines.[47,48] For instance, siRNA-mediated lncRNA ANCR inhibition promotes osteoblast differentiation in the human fetal osteoblastic cell line hFOB1.19,[49] whereas, silencing of lncRNA NONHSAT009968 reduces the staphylococcal protein A-inhibited osteogenic differentiation in human bone mesenchymal stem cells.[50] To the best of our knowledge, this is the first report to show that knockdown of TUG1 significantly inhibited osteoblast differentiation by targeting miR-204-5p/Runx2 axis *in vitro*. These promising data and our current findings demonstrate that lncRNAs indeed play a critical role in osteoblast differentiation. Nevertheless, further studies are needed to establish a direct link between lncRNAs and other identified signalling pathways participating in osteogenic differentiation in the context of CAVD.

4.1 Limitations

Our study has several limitations. First, we only explored the miRNA sponge function of TUG1 in cytoplasm. It should be noted that, apart from cell cytoplasm, TUG1 is also expressed in the nucleus of VICs. Further work is necessary to investigate more functions of TUG1 in the nucleus. Second, we only identified that TUG1 could positively regulate Runx2 expression at the post-transcriptional level through sponging miR-204-5p in VICs. Whether TUG1 could function as a sponge lncRNA to affect expressions of other key regulators in CAVD may need further investigation. Third, we did not provide evidence suggesting that the TUG1-transgenic mice may develop aortic valve calcification. Nonetheless, the present findings in human calcified aortic valves and primary human aortic VICs generate novel hypotheses about the role of TUG1 in CAVD.

4.2 Conclusion

In the present study, we identify TUG1 as a novel positive regulator of osteogenic differentiation in CAVD pathogenesis. Moreover, our findings shed light on the interaction between TUG1 and miR-204-5p in CAVD, and reveal that TUG1 positively regulates post-transcriptional expression of Runx2 by sponging miR-204-5p in CAVD. Knockdown of TUG1 via RNAi or GapmeR decreased Runx2 expression, leading to inhibition of osteogenic differentiation by down-regulation of osteogenic-specific protein levels (osteocalcin, osteopontin, and osterix), providing a novel therapeutic target for CAVD.

Supplementary material

Supplementary material is available at *Cardiovascular Research* online.

Conflict of interest: none declared.

Funding

This work was supported by the National Natural Science Foundation of China [81500300 to W.Y.J.]; and the National Key Research and Development Program of China [2016YFA0101100 to D.N.G.].

References

1. Bonow RO, Leon MB, Doshi D, Moat N. Management strategies and future challenges for aortic valve disease. *Lancet* 2016;**387**:1312–1323.
2. Towler DA. Molecular and cellular aspects of calcific aortic valve disease. *Circ Res* 2013;**113**:198–208.
3. Yutzey KE, Demer LL, Body SC, Huggins GS, Towler DA, Giachelli CM, Hofmann-Bowman MA, Mortlock DP, Rogers MB, Sadeghi MM, Aikawa E. Calcific aortic valve disease: a consensus summary from the Alliance of Investigators on Calcific Aortic Valve Disease. *Arterioscler Thromb Vasc Biol* 2014;**34**:2387–2393.

4. Poggio P, Sainger R, Branchetti E, Grau JB, Lai EK, Gorman RC, Sacks MS, Parolari A, Bavaria JE, Ferrari G. Noggin attenuates the osteogenic activation of human valve interstitial cells in aortic valve sclerosis. *Cardiovasc Res* 2013;**98**:402–410.
5. An integrated encyclopedia of DNA elements in the human genome. *Nature* 2012; **489**:57–74.
6. Nagano T, Fraser P. No-nonsense functions for long noncoding RNAs. *Cell* 2011; **145**:178–181.
7. Cabili MN, Dunagin MC, McClanahan PD, Biaesch A, Padovan-Merhar O, Regev A, Rinn JL, Raj A. Localization and abundance analysis of human lncRNAs at single-cell and single-molecule resolution. *Genome Biol* 2015;**16**:20.
8. Liu SJ, Nowakowski TJ, Pollen AA, Lui JH, Horlbeck MA, Attenello FJ, He D, Weissman JS, Kriegstein AR, Diaz AA, Lim DA. Single-cell analysis of long non-coding RNAs in the developing human neocortex. *Genome Biol* 2016;**17**:67.
9. Wang P, Xue Y, Han Y, Lin L, Wu C, Xu S, Jiang Z, Xu J, Liu Q, Cao X. The STAT3-binding long noncoding RNA lnc-DC controls human dendritic cell differentiation. *Science* 2014;**344**:310–313.
10. Huang ZP, Ding Y, Chen J, Wu G, Kataoka M, Hu Y, Yang JH, Liu J, Drakos SG, Selzman CH, Kyselovic J, Qu LH, Dos Remedios CG, Pu WT, Wang DZ. Long non-coding RNAs link extracellular matrix gene expression to ischemic cardiomyopathy. *Cardiovasc Res* 2016;**112**:543–554.
11. Uchida S, Dimmeler S. Long noncoding RNAs in cardiovascular diseases. *Circ Res* 2015;**116**:737–750.
12. Bar C, Chatterjee S, Thum T. Long noncoding RNAs in cardiovascular pathology, diagnosis, and therapy. *Circulation* 2016;**134**:1484–1499.
13. Greco S, Zaccagnini G, Fuschi P, Voellenkle C, Carrara M, Sadeghi I, Bearzi C, Maimone B, Castelvecchio S, Stellos K, Gaetano C, Menicanti L, Martelli F. Increased BACE1-AS long noncoding RNA and beta-amyloid levels in heart failure. *Cardiovasc Res* 2017;**113**:453–463.
14. Viereck J, Kumarswamy R, Foinquinos A, Xiao K, Avramopoulos P, Kunz M, Dittrich M, Maetzig T, Zimmer K, Remke J, Just A, Fendrich J, Scherf K, Bolesani E, Schambach A, Weidemann F, Zweigerdt R, de Windt LJ, Engelhardt S, Dandekar T, Batkai S, Thum T. Long noncoding RNA Chast promotes cardiac remodeling. *Sci Transl Med* 2016;**8**:326ra322.
15. Wang Z, Zhang XJ, Ji YX, Zhang P, Deng KQ, Gong J, Ren S, Wang X, Chen I, Wang H, Gao C, Yokota T, Ang YS, Li S, Cass A, Vondriska TM, Li G, Deb A, Srivastava D, Yang HT, Xiao X, Li H, Wang Y. The long noncoding RNA Chaer defines an epigenetic checkpoint in cardiac hypertrophy. *Nat Med* 2016;**22**:1131–1139.
16. Young TL, Matsuda T, Cepko CL. The noncoding RNA taurine upregulated gene 1 is required for differentiation of the murine retina. *Curr Biol* 2005;**15**:501–512.
17. Niu Y, Ma F, Huang W, Fang S, Li M, Wei T, Guo L. Long non-coding RNA TUG1 is involved in cell growth and chemoresistance of small cell lung cancer by regulating LIMK2b via EZH2. *Mol Cancer* 2017;**16**:5.
18. Zhang E, He X, Yin D, Han L, Qiu M, Xu T, Xia R, Xu L, Yin R, De W. Increased expression of long noncoding RNA TUG1 predicts a poor prognosis of gastric cancer and regulates cell proliferation by epigenetically silencing of p57. *Cell Death Dis* 2016;**7**:e2109.
19. Chen C, Cheng G, Yang X, Li C, Shi R, Zhao N. Tanshinol suppresses endothelial cells apoptosis in mice with atherosclerosis via lncRNA TUG1 up-regulating the expression of miR-26a. *Am J Transl Res* 2016;**8**:2981–2991.
20. Lee JT. Epigenetic regulation by long noncoding RNAs. *Science* 2012;**338**:1435–1439.
21. Engreitz JM, Ollikainen N, Guttman M. Long non-coding RNAs: spatial amplifiers that control nuclear structure and gene expression. *Nat Rev Mol Cell Biol* 2016;**17**:756–770.
22. Thomson DW, Dinger ME. Endogenous microRNA sponges: evidence and controversy. *Nat Rev Genet* 2016;**17**:272–283.
23. Katsushima K, Natsume A, Ohka F, Shinjo K, Hatanaka A, Ichimura N, Sato S, Takahashi S, Kimura H, Totoki Y, Shibata T, Naito M, Kim HJ, Miyata K, Kataoka K, Kondo Y. Targeting the Notch-regulated non-coding RNA TUG1 for glioma treatment. *Nat Commun* 2016;**7**:13616.
24. Cai H, Liu X, Zheng J, Xue Y, Ma J, Li Z, Xi Z, Li Z, Bao M, Liu Y. Long non-coding RNA taurine upregulated 1 enhances tumor-induced angiogenesis through inhibiting microRNA-299 in human glioblastoma. *Oncogene* 2017;**36**:318–331.
25. Li F, Yao Q, Ao L, Cleveland JC Jr, Dong N, Fullerton DA, Meng X. Klotho suppresses high phosphate-induced osteogenic responses in human aortic valve interstitial cells through inhibition of Sox9. *J Mol Med* 2017;**95**:739–751.
26. Xiao X, Zhou T, Guo S, Guo C, Zhang Q, Dong N, Wang Y. LncRNA MALAT1 sponges miR-204 to promote osteoblast differentiation of human aortic valve interstitial cells through up-regulating Smad4. *Int J Cardiol* 2017;**243**:404–412.
27. Zhang A, Zhou N, Huang J, Liu Q, Fukuda K, Ma D, Lu Z, Bai C, Watabe K, Mo YY. The human long non-coding RNA-RoR is a p53 repressor in response to DNA damage. *Cell Res* 2013;**23**:340–350.
28. Rajamannan NM. The role of Lrp5/6 in cardiac valve disease: experimental hypercholesterolemia in the ApoE-/-/Lrp5-/- mice. *J Cell Biochem* 2011;**112**:2987–2991.
29. Quinn JJ, Chang HY. Unique features of long non-coding RNA biogenesis and function. *Nat Rev Genet* 2016;**17**:47–62.
30. Gregory RI, Chendrimada TP, Cooch N, Shiekhattar R. Human RISC couples microRNA biogenesis and posttranscriptional gene silencing. *Cell* 2005;**123**:631–640.
31. Wirrig EE, Hinton RB, Yutzey KE. Differential expression of cartilage and bone-related proteins in pediatric and adult diseased aortic valves. *J Mol Cell Cardiol* 2011; **50**:561–569.
32. Carrion K, Dyo J, Patel V, Sasik R, Mohamed SA, Hardiman G, Nigam V, Alamo J. C D. The long non-coding HOTAIR is modulated by cyclic stretch and WNT/beta-CATENIN in human aortic valve cells and is a novel repressor of calcification genes. *PloS One* 2014;**9**:e96577.
33. Hadji F, Boulanger M-C, Guay S-P, Gaudreault N, Amellah S, Mkannez G, Bouchareb R, Marchand JT, Nsaibia MJ, Guauque-Olarte S, Pibarot P, Bouchard L, Bossé Y, Mathieu P. Altered DNA methylation of long noncoding RNA H19 in calcific aortic valve disease promotes mineralization by silencing NOTCH1. *Circulation* 2016;**134**: 1848–1862.
34. Fort A, Hashimoto K, Yamada D, Salimullah M, Keya CA, Saxena A, Bonetti A, Voineagu I, Bertin N, Kratz A, Noro Y, Wong CH, de Hoon M, Andersson R, Sandelin A, Suzuki H, Wei CL, Koseki H, Hasegawa Y, Forrest AR, Carninci P. Deep transcriptome profiling of mammalian stem cells supports a regulatory role for retrotransposons in pluripotency maintenance. *Nat Genet* 2014;**46**:558–566.
35. Derrien T, Johnson R, Bussotti G, Tanzer A, Djebali S, Tilgner H, Guernec G, Martin D, Merkel A, Knowles DG, Lagarde J, Veeravalli L, Ruan X, Ruan Y, Lassmann T, Carninci P, Brown JB, Lipovich L, Gonzalez JM, Thomas M, Davis CA, Shiekhattar R, Gingeras TR, Hubbard TJ, Notredame C, Harrow J, Guigo R. The GENCODE v7 catalog of human long noncoding RNAs: analysis of their gene structure, evolution, and expression. *Genome Res* 2012;**22**:1775–1789.
36. Salmena L, Poliseno L, Tay Y, Kats L, Pandolfi PP. A ceRNA hypothesis: the Rosetta Stone of a hidden RNA language? *Cell* 2011;**146**:353–358.
37. Rashid F, Shah A, Shan G. Long non-coding RNAs in the cytoplasm. *Genom Proteom Bioinform* 2016;**14**:73–80.
38. Zhang E, Han L, Yin D, He X, Hong L, Si X, Qiu M, Xu T, De W, Xu L, Shu Y, Chen J. H3K27 acetylation activated-long non-coding RNA CCAT1 affects cell proliferation and migration by regulating SPRY4 and HOXB13 expression in esophageal squamous cell carcinoma. *Nucleic Acids Res* 2017;**45**:3086–3101.
39. Cai Z, Li F, Gong W, Liu W, Duan Q, Chen C, Ni L, Xia Y, Cianflone K, Dong N, Wang DW. Endoplasmic reticulum stress participates in aortic valve calcification in hypercholesterolemic animals. *Arterioscler Thromb Vasc Biol* 2013;**33**:2345–2354.
40. Johnson RC, Leopold JA, Loscalzo J. Vascular calcification: pathobiological mechanisms and clinical implications. *Circ Res* 2006;**99**:1044–1059.
41. Zhang XW, Zhang BY, Wang SW, Gong DJ, Han L, Xu ZY, Liu XH. Twist-related protein 1 negatively regulated osteoblastic transdifferentiation of human aortic valve interstitial cells by directly inhibiting runt-related transcription factor 2. *J Thorac Cardiovasc Surg* 2014;**148**:1700–1708.e1701.
42. Branchetti E, Sainger R, Poggio P, Grau JB, Patterson-Fortin J, Bavaria JE, Chorny M, Lai E, Gorman RC, Levy RJ, Ferrari G. Antioxidant enzymes reduce DNA damage and early activation of valvular interstitial cells in aortic valve sclerosis. *Arterioscler Thromb Vasc Biol* 2013;**33**:e66–e74.
43. Wang Y, Chen S, Deng C, Li F, Wang Y, Hu X, Shi F, Dong N. MicroRNA-204 targets Runx2 to attenuate BMP-2-induced osteoblast differentiation of human aortic valve interstitial cells. *J Cardiovasc Pharmacol* 2015;**66**:63–71.
44. Xia T, Liao Q, Jiang X, Shao Y, Xiao B, Xi Y, Guo J. Long noncoding RNA associated-competing endogenous RNAs in gastric cancer. *Sci Rep* 2014;**4**:6088.
45. Du Z, Sun T, Hacisuleyman E, Fei T, Wang X, Brown M, Rinn JL, Lee MG, Chen Y, Kantoff PW, Liu XS. Integrative analyses reveal a long noncoding RNA-mediated sponge regulatory network in prostate cancer. *Nat Comms* 2016;**7**:10982.
46. Freeman RV, Otto CM. Spectrum of calcific aortic valve disease: pathogenesis, disease progression, and treatment strategies. *Circulation* 2005;**111**:3316–3326.
47. Huang Y, Zheng Y, Jia L, Li W. Long noncoding RNA H19 promotes osteoblast differentiation via TGF-beta1/Smad3/HDAC signaling pathway by deriving miR-675. *Stem Cells* 2015;**33**:3481–3492.
48. Lee DF, Su J, Kim HS, Chang B, Papatsenko D, Zhao R, Yuan Y, Gingold J, Xia W, Darr H, Mirzayans R, Hung MC, Schaniel C, Lemischka IR. Modeling familial cancer with induced pluripotent stem cells. *Cell* 2015;**161**:240–254.
49. Zhu L, Xu PC. Downregulated LncRNA-ANCR promotes osteoblast differentiation by targeting EZH2 and regulating Runx2 expression. *Biochem Biophys Res Commun* 2013;**432**:612–617.
50. Cui Y, Lu S, Tan H, Li J, Zhu M, Xu Y. Silencing of long non-coding RNA NONHSAT009968 ameliorates the staphylococcal protein A-inhibited osteogenic differentiation in human bone mesenchymal stem cells. *Cell Physiol Biochem* 2016;**39**: 1347–1359.